Biomass Waste-Derived Microporous Carbons with Controlled Texture and Enhanced Hydrogen Uptake

Fangyi Cheng, Jing Liang, Jianzhi Zhao, Zhanliang Tao, and Jun Chen*

Key Laboratory of Energy-Material Chemistry (Tianjin) and Engineering Research Center of Energy Storage & Conversion (Ministry of Education), College of Chemistry, Nankai University, Tianjin 300071, P.R. China

Received September 30, 2007. Revised Manuscript Received December 14, 2007

We report on the facile preparation of biomass waste-derived microporous carbons and the investigation of their hydrogen storage performance. By adjusting the reaction parameters, different carbon materials with controlled morphology and texture were prepared through the carbonization and activation of the hydrolytic lignin from inexpensive biomass waste. The as-obtained samples were characterized using instrumental analyses such as SEM, TEM, EDX, XRD, IR, ICP, and XPS. It was found that the as-synthesized microporous carbons exhibited high surface area (2000−3100 $m^2\ g^{-1}$), large micropore volume (1.11−1.68 $cm^3\ g^{-1}$), and narrow pore size distribution (0.77−0.91 nm). Furthermore, a considerable hydrogen uptake exceeding 5 wt % with an isosteric adsorption heat of 4.1−7.5 kJ mol^{-1} was attained with the microporous carbons, showing their potential usage in compacting gaseous fuels of hydrogen.

1. Introduction

Current concerns of increasing energy shortage and environmental issues have initiated extensive efforts toward the more efficient utilization of biomass, which constitutes one of the most abundant renewable resources on earth and contributes to the reduction of net CO_2 emission.[1–3] It has been shown that biomass is promising to be economically converted to chemicals and biofuels, including liquid bioethanol and biodiesel as well as gaseous hydrogen and alkanes.[4–6] However, enormous quantities of biomass resources and especially biomass wastes that mainly derive from agricultural residues and forest byproducts have been traditionally discarded or simply combusted to generate heat for thermal applications. This situation contradicts the requirement of sustainable development for modern society and thus needs to be improved. Therefore, exploring the added value of biomass wastes is of great importance to meet sustainable goals.

Generally, gasification, pyrolysis, and hydrolysis are typical routes proposed for the systematical application of biomass.[1a] Producing syngas and bio-oils from the gasification and liquefaction routes has been well established, whereas the hydrolysis pathway is currently under extensive development.[6] The hydrolysis route might outperform the gasification and liquefaction pathway due to low energy consumption and diverse biological and chemical processing on the intermediate product.[7] However, lignin, one of the major hydrolytic products, is thrown away in many practical cases such as pulp industry and biorefinery. Thus, production of valuable byproduct should also be integrated in the hydrolysis process, making the whole concept more economically profitable. Lignin and chars from the hydrolysis of biomass wastes contain abundant carbon and therefore can serve as an inexpensive resource to prepare activated carbons, which are versatile sorbents and show wide applications in many economic sectors and concern areas such as food, environment, chemistry, energy, and so on.[8]

Hydrogen is considered to be a clean energy carrier, while the main challenge facing the anticipated hydrogen economy is the lack of effective storage media despite its abundance and the diverse existing routes for its production.[9] The study on hydrogen storage is to search alternative effective materials/technologies with proper thermodynamics and kinetics for reversible hydrogen sorption and desorption.[10–12] As an example, hydrogen storage in carbonaceous materials has received extensive interest as a result of the advantages

* Corresponding author. E-mail: chenabc@nankai.edu.cn.

(1) (a) Huber, G. W.; Iborra, S.; Corma, A. *Chem. Rev.* **2006**, *106*, 4044. (b) Klass, D. L. *Biomass for Renewable Energy, Fuels, and Chemicals*; Academic Press: New York, 1998.
(2) (a) Titirici, M. M.; Thomas, A.; Yu, S. H.; Mueller, J. O.; Antonietti, M. *Chem. Mater.* **2007**, *19*, 4205. (b) Demirbas, A. *Prog. Energy Combust. Sci.* **2007**, *33*, 1. (c) Ni, M.; Leung, D. Y. C.; Leung, M. K. H.; Sumathy, K. *Fuel Process. Technol.* **2006**, *87*, 461.
(3) (a) Tilman, D.; Hill, J.; Lehman, C. *Science* **2006**, *314*, 1598. (b) Farrell, A. E.; Plevin, R. J.; Turner, B. T.; Jones, A. D.; O'Hare, M.; Kammen, D. M. *Science* **2006**, *311*, 506.
(4) (a) Corma, A.; Iborra, S.; Velty, A. *Chem. Rev.* **2007**, *107*, 2411. (b) Yan, N.; Zhao, C.; Luo, C.; Dyson, P. J.; Liu, H.; Kou, Y. *J. Am. Chem. Soc.* **2006**, *128*, 8714. (c) Swierczynski, D.; Courson, C.; Bedel, L.; Kiennemann, A.; Guille, J. *Chem. Mater.* **2006**, *18*, 4025.
(5) (a) Cortright, R. D.; Davda, R. R.; Dumesic, J. A. *Nature* **2002**, *418*, 964. (b) Roman-Leshkov, Y.; Barrett, C. J.; Liu, Z. Y.; Dumesic, J. A. *Nature* **2007**, *447*, 982.
(6) Navarro, R. M.; Peña, M. A.; Fierro, J. L. G. *Chem. Rev.* **2007**, *107*, 3952.
(7) Hamelinck, C. N.; van Hooijdonk, G.; Faaij, A. *Biomass Bioenergy* **2005**, *28*, 384.
(8) (a) Barsukov, I. V.; Johnson, C. S.; Doninger, J. E.; Barsukov, V. Z. *New Carbon Based Materials for Electrochemical Energy Storage Systems: Batteries, Supercapacitors and Fuel Cells*; Springer: Dordrecht, 2003. (b) Bandosz, T. J.; Seredych, M.; Allen, J.; Wood, J.; Rosenberg, E. *Chem. Mater.* **2007**, *19*, 2500. (c) Ariga, K.; Vinu, A.; Miyahara, M.; Hill, J. P.; Mori, T. *J. Am. Chem. Soc.* **2007**, *129*, 11022. (d) Ohkubo, T.; Konish, T.; Hattori, Y.; Kanoh, H.; Fujikawa, T.; Kaneko, K. *J. Am. Chem. Soc.* **2002**, *124*, 11860.
(9) Schlapbach, L.; Züttel, A. *Nature* **2001**, *414*, 353.

10.1021/cm702816x CCC: $40.75 © 2008 American Chemical Society
Published on Web 01/25/2008

associated with their low mass density and the reversibility of physisorption.[13] On one hand, the reported experimental and computational results often show discrepancy regarding the H_2 storage capacity among different carbon-based materials, owing to insufficient characterization of them.[14] On the other hand, carbonaceous adsorbents possessing high surface areas, tuned pore structures, and modified H_2-C interactions continue to attract scientific and technical interest. Recently, carbon nanostructures and template-synthesized porous carbon materials have been prepared and demonstrated to be promising candidates for H_2-storage applications.[15–17] However, there are some inherent drawbacks associated with the widespread application of nanostructured carbons and template-directed porous carbons because their synthesis is usually costly and requires relatively complicated manipulation or special facility.

In this work, we focus on the facile preparation and detailed characterization of microporous carbons and investigate the hydrogen storage capability of such inexpensive carbonaceous materials. First, we demonstrate that microporous carbons with controlled morphologies and textures can be prepared from low-cost biomass wastes. Second, the as-synthesized carbons possess high surface areas, large pore volumes, and narrow pore size distribution, and in addition, they show superior adsorption performance over carbon nanotubes with respect to cryogenic hydrogen uptake. Therefore, the present study not only proposes a possible route for the higher-value use of biomass wastes but also illustrates the relationship between the porous structure of the biomass-derived carbons and the enhanced hydrogen storage capacity.

2. Experimental Section

Synthesis. Active carbon samples were prepared by carbonization and activation of the hydrolytic product of sawdust. Detailed procedures are described as follows. First, sawdust (volatile matter, 65.2 wt %; ash content, 1.1 wt %) obtained from a wood processing factory was ground and sieved to collect the powders with typical size of less than 0.1 mm. Second, 2.5 g of the collected powders and 40 mL of dilute acid were loaded in a 50 mL autoclave. After thorough magnetic stirring, the autoclave was sealed and maintained at 110 °C for 6 h and then allowed to cool to room temperature. Third, the resulting hydrolytic solid was collected, washed, and dried under a vacuum to obtain a dark-color precursor, which contains approximately 2.0 wt % ash content, 5.3 wt % alcohol−benzene (v/v = 1) extracted substance, 6.8 wt % cellulose, and 80.6 wt % lignin. Finally, experimental setup for the preparation of active carbon was based on a vertically located furnace system, which was equipped with a removable reactor and three control inlets and outlets. The as-prepared products were hereafter designated as **BW-A**, **BW-B**, **BW-C**, and **BW-D**. Among them, sample **BW-A** was prepared by first carbonizing the precursor at 550 °C for 1 h and then activating it at 800 °C for 1 h in a flowing mixed gas of steam and carbon dioxide (v/v = 1). The heating rate from the starting temperature to the set temperature was 5 °C min^{-1} for **BW-A** and 10 °C min^{-1} for the other three. Similar procedures were carried out for sample **BW-B** except that the carbonization temperature was set at 600 °C. Sample **BW-C** was obtained by carbonizing the precursor at 650 °C for 1 h and activating it at 850 °C for 1.5 h. As a comparison, sample **BW-D** was prepared by chemical activation with KOH. In detail, the precursor was impregnated with KOH aqueous solution (precursor/KOH = 1, in weight) and then dried at 105 °C to form an impregnated mixture, which was heated at 780 °C for 1.5 h under argon flow. After that, the resulting solid was thoroughly washed with water and finally dried under vacuum.

Characterization. The obtained carbon samples were evacuated at 383 K under vacuum for 6 h before characterization. The morphologies of the samples were characterized by scanning electron microscopy (SEM, Philips XL-30 and JEOL JSM-6700F Field Emission) equipped with energy dispersive X-ray spectroscopy (EDX) and transmission electron microscopy (TEM, FEI Tecnai 20 operating at 200 kV). The composition and structure was analyzed using inductively coupled plasma (ICP) emission spectroscopy (Thermo Jarrell-Ash Corp.), powder X-ray diffraction (XRD, Rigaku D/max-2500 diffractometer with Cu Kα radiation), X-ray photoelectron spectroscopy (XPS, Kratos Axis Ultra DLD spectrometer with Al Kα X-ray source), and Fourier transform infrared (FTIR) spectroscopy (Bruker Tensor 27 spectrometer in the range of 500–4000 cm^{-1} on sample pellets made with KBr). Textural properties were determined by nitrogen and argon sorption on a Micromeritics ASAP 2020 sorptometer. The specific surface areas were calculated from the N_2 adsorption data in the partial pressure (P/P_0) range 0.02–0.25 according to Brunauer–Emmett–Teller (BET) theory, and the pore size distribution (PSD) curves were based on the Horvath–Kawazoe (HK) model assuming a slit pore shape.[16]

Hydrogen Storage Test. Gravimetric determination of hydrogen storage capacity was carried out on an Intelligent Gravimetric Analyzer (IGA001, Hiden Isochema).[18] All samples (30−50 mg) were evacuated to ultrahigh vacuum at 110 °C overnight before the test. Hydrogen sorption measurements were performed at cryogenic temperatures over the pressure range of 0–10 bar. High-

(10) (a) Wang, X. F.; Andrews, L. *Angew. Chem., Int. Ed.* **2007**, *46*, 2602. (b) Germain, J.; Hradil, J.; Frechet, J. M. J.; Svec, F. *Chem. Mater.* **2006**, *18*, 4430. (c) Hu, X.; Skadtchenko, B. O.; Trudeau, M.; Antonelli, D. M. *J. Am. Chem. Soc.* **2006**, *128*, 11740. (d) Seayad, A. M.; Antonelli, D. M. *Adv. Mater.* **2004**, *16*, 765.

(11) (a) Wu, H.; Zhou, W.; Udovic, T. J.; Rush, J. J. *Chem. Mater.* **2007**, *19*, 329. (b) Grochala, W.; Edwards, P. P. *Chem. Rev.* **2004**, *104*, 1283. (c) Chen, J.; Li, S. L.; Tao, Z. L.; Shen, Y. T.; Cui, C. X. *J. Am. Chem. Soc.* **2003**, *125*, 5284. (d) Chen, P.; Xiong, Z. T.; Luo, J. Z.; Lin, J. Y.; Tan, L. *Nature* **2002**, *420*, 302. (e) Chen, J.; Kuriyama, N.; Xu, Q.; Takeshita, H. T.; Sakai, T. *J. Phys. Chem. B* **2001**, *105*, 11214.

(12) (a) Siberio-Perez, D. Y.; Wong-Foy, A. G.; Yaghi, O. M.; Matzger, A. J. *Chem. Mater.* **2007**, *19*, 3681. (b) Park, H.; Britten, J. F.; Mueller, U.; Lee, J. Y.; Li, J.; Parise, J. B. *Chem. Mater.* **2007**, *19*, 1302. (c) Forster, P. M.; Eckert, J.; Heiken, B. D.; Parise, J. B.; Yoon, J. W.; Jhung, S. H.; Chang, J. S.; Cheetham, A. K. *J. Am. Chem. Soc.* **2006**, *128*, 16846. (d) Kaye, S. S.; Long, J. R. *J. Am. Chem. Soc.* **2005**, *127*, 6506.

(13) Nijkamp, M. G.; Raaymakers, J. E. M. J.; Van Dillen, A. J.; De Jong, K. P. *Appl. Phys. A: Mater. Sci. Process.* **2001**, *72*, 619.

(14) (a) Bhatia, S. K.; Myers, A. L. *Langmuir* **2006**, *22*, 1688. (b) Panella, B.; Hirscher, M.; Roth, S. *Carbon* **2005**, *43*, 2209. (c) Züttel, A.; Nüzenadel, C.; Sudan, P.; Mauron, P.; Emmenegger, C.; Rentsch, S.; Schlapbach, L.; Weidenkaff, A.; Kiyobayashi, T. *J. Alloys Compd.* **2002**, *330–332*, 676.

(15) (a) Miyamoto, J.; Hattori, Y.; Noguchi, D.; Tanaka, H.; Ohba, T.; Utsumi, S.; Kanoh, H.; Kim, Y. A.; Muramatsu, H.; Hayashi, T.; Endo, M.; Kaneko, K. *J. Am. Chem. Soc.* **2006**, *128*, 12636. (b) Lueking, A. D.; Gutierrez, H. R.; Fonseca, D. A.; Naryanan, D. L.; Essendelft, D. V.; Jain, P.; Clifford, C. E. B. *J. Am. Chem. Soc.* **2006**, *128*, 7758. (c) Liang, C.; Dai, S. *J. Am. Chem. Soc.* **2006**, *128*, 5316. (d) Dillon, A. C.; Jones, K. M.; Bekkedahl, T. A.; Kiang, C. H.; Bethune, D. S.; Heben, M. J. *Nature* **1997**, *386*, 377.

(16) Yang, Z.; Xia, Y.; Mokaya, R. *J. Am. Chem. Soc.* **2007**, *129*, 1673.

(17) (a) Gogotsi, Y.; Dash, R. K.; Yushin, G.; Yildirim, T.; Laudisio, G.; Fischer, J. E. *J. Am. Chem. Soc.* **2005**, *127*, 16006. (b) Yushin, G.; Dash, R.; Jagiello, J.; Fischer, J. E.; Gogotsi, Y. *Adv. Funct. Mater.* **2006**, *16*, 2288.

(18) (a) Zhao, X. B.; Xiao, B.; Fletcher, A. J.; Thomas, K. M. *J. Phys. Chem. B* **2005**, *109*, 8880. (b) Li, W. Y.; Li, C. S.; Ma, H.; Chen, J. *J. Am. Chem. Soc.* **2007**, *129*, 6710.

Scheme 1. Proposed Route Showing the High-Value Use of Biomass Wastes and Depicting the Synthesis Process of Microporous Carbons

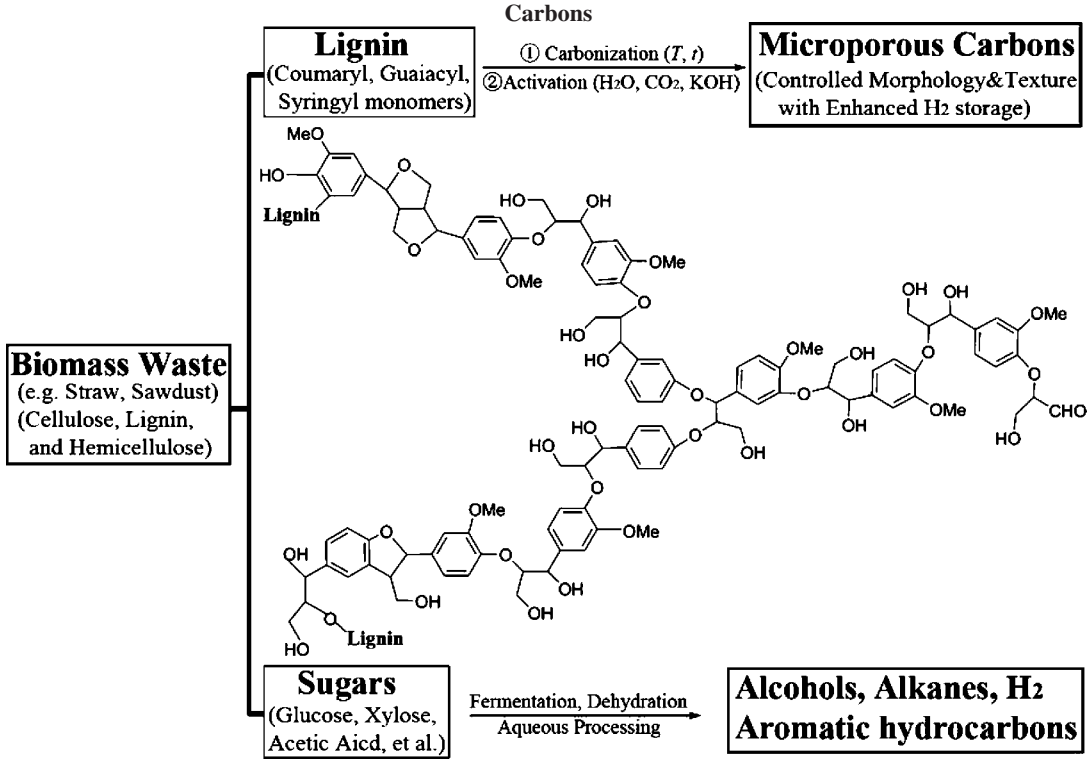

purity hydrogen (>99.999%, supplied by Air Products Tianjin Inc.) with additional moisture removal was used throughout the H_2 uptake tests. Carbon density of 1.56 g cm^{-3} (determined from He adsorption isotherms at 30 °C) and hydrogen density of 0.04 g cm^{-3} were used for buoyancy correction, while 0.077 g cm^{-3} was used for the density of adsorbed hydrogen.[16,18a] The hydrogen uptake of commercial activated carbon (AX-21, Anderson) and multiwalled carbon nanotubes (prepared according to previous literature[19]) was also measured as a comparison in the controlled experiment. The isosteric heat (Q_{st}) of H_2 adsorption was calculated using Clausius−Clapeyron equation:

$$\left(\frac{\partial \ln p}{\partial \ln T}\right)_\theta = \frac{Q_{st}}{RT^2} \quad (1)$$

where R is the universal gas constant and θ is the coverage fraction at a given pressure P and temperature T. For a certain θ value, Q_{st} was obtained by applying the integrated form of eq 1:

$$Q_{st} = \frac{T_1 T_2}{T_2 - T_1}\left(\ln \frac{P_2}{P_1}\right) \quad (2)$$

where P_1 and P_2 are the equilibrium pressure at temperatures T_1 and T_2, respectively. In our study, the temperatures of liquid nitrogen and argon were selected as T_1 and T_2, respectively.

3. Results and Discussion

3.1. Synthesis and Characterization. A possible route for the higher-value use of biomass waste is shown in Scheme 1. In general, biomass waste such as straw and sawdust can be hydrothermally decomposed into lignin and sugars. The aqueous hydrolytic product including glucose, xylose, and acetic acid can be further converted to liquid and gaseous fuels (e.g., alcohols, alkanes, H_2, etc.) through fermentation, dehydration, or other aqueous processing techniques. Detailed description along this line has been reviewed elsewhere[4,6] and is thus beyond the scope of this work. We employ the hydrolytic lignin as an abundant and inexpensive precursor to prepare microporous carbons, which can find wide application in different fields ranging from catalyst to energy storage and conversion.

Figure 1 shows the SEM image of the precursor, displaying irregular shape and size. Both microspheres and splitted fibers can be observed, indicating that the hydrothermal treatment has broken up the initial structure of the raw materials. The surface of the solid appears to be relatively compact and rough with no apparently observed holes or cavities. In addition, the XRD pattern of the solid precursor shows amorphous character (data not shown). These observations reflect the features of lignin, which is an irregular branched and substituted aromatic polymer (see Scheme 1) and functions as the support in cell walls of plants.[1a] The major component in the hydrolytic solid from biomass waste is lignin, and the total carbon content reaches 65 wt %, rendering it a suitable precursor for preparing active carbons.

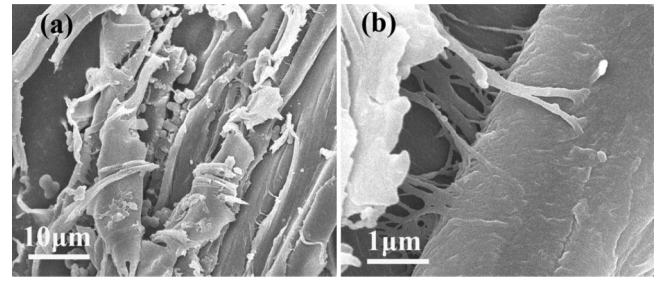

Figure 1. SEM images of the hydrolytic solid from biomass waste employed as the precursor for preparing active carbons.

(19) Wang, W.; Poudel, B.; Wang, D. Z.; Ren, Z. F. *J. Am. Chem. Soc.* **2005**, *127*, 18019.

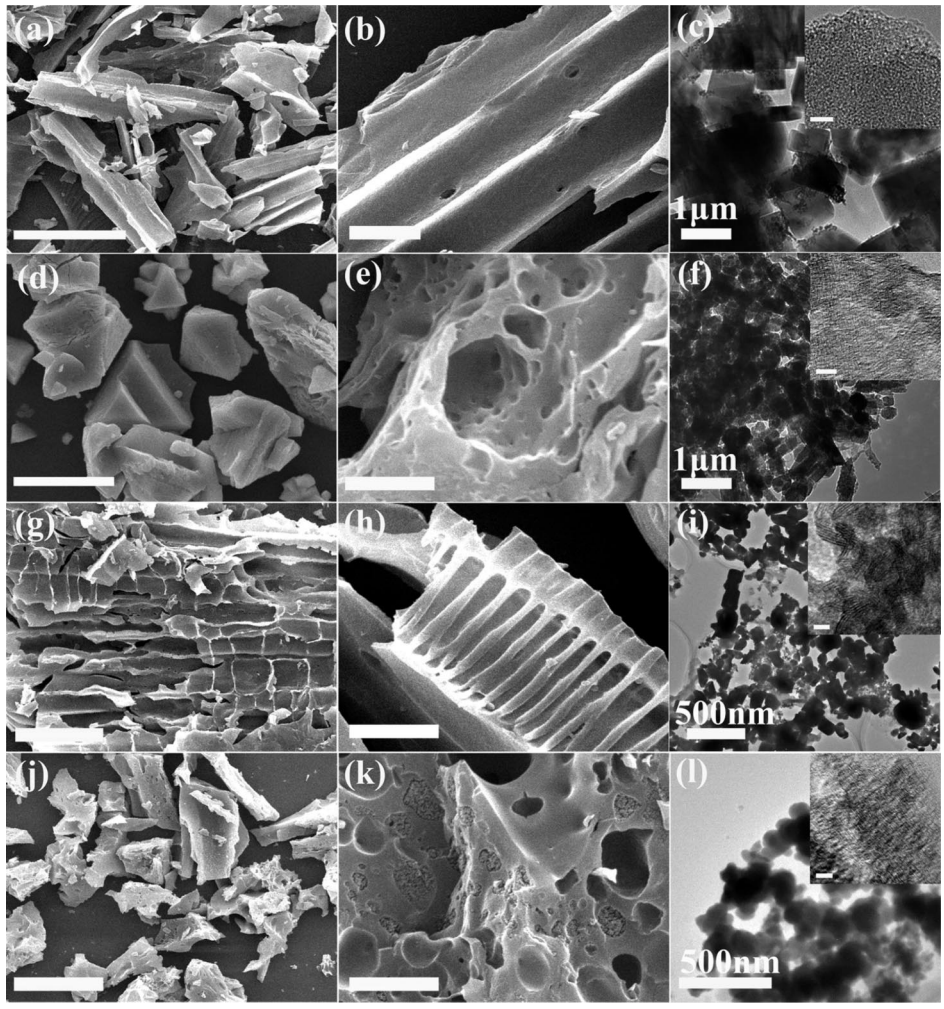

Figure 2. SEM (a and b, d and e, g and h, j and k) and TEM (c, f, i, l) images of the obtained microporous carbons prepared from biomass wastes. a−c, d−f, g−i, and j−l correspond to samples **BW-A**, **BW-B**, **BW-C**, and **BW-D**, respectively. Insets in c, f, i, and l show the HRTEM images of **BW-A**, **BW-B**, **BW-C**, and **BW-D**. Scale bars: (a, d, g, j) 50 μm, (b, e, h, k) 5 μm, inset of (c, f, i, l) 10 nm.

Figure 2 shows the SEM and TEM images of the as-prepared four carbon materials. The samples activated by H_2O and CO_2 (samples **BD-A**, **BD-B**, and **BD-C**) exhibit smooth surfaces with irregularly shaped holes on them. From **BW-A** to **BW-C**, the carbon surface appears to be more etched with elevated carbonization temperature and prolonged activation time. A lower carbonization/activation temperature has resulted in carbons with relatively less eroded cavities and higher yield of product accordingly. Under the circumstance of elevated temperature and prolonged dwell time, the activating agents react more vigorously with the precursor, leading to well developed porous carbon structures.

When activating the hydrolytic solid with KOH, the resulting sample **BW-D** contains both open holes and holes filled with aggregating nanoparticles, as shown in Figure 2k. The particles within the holes consist of carbon, as determined by EDX analysis (shown in Figure 3a infra). These disorganized carbon nanoparticles may derive from the decomposition of tarry matter during carbonization process. Low-magnification TEM images (Figure 2c,f,i,l) show a much larger average particle size of sample **BW-A** than that of the other three samples. This observation indicates that **BW-A** is less prone to be dispersed by ultrasonic treatment and thus confirms the intensive influence of carbonization/activation condition on the carbon structure. Numerous slit-shaped micropores along with a few irregular mesopores can be found in the HRTEM images (Figure 2c,f,i,l). In addition, the ordered carbon microstructures with obvious defects were observed. Therefore, SEM together with TEM characterization clearly reveals that carbons with diverse morphologies can be prepared from biomass waste.

XRD, EDX, FTIR, and XPS spectra (Figure 3) were further carried out to analyze the composition and structure of the samples. The EDX spectrum in Figure 3a shows the elemental composition. The presence of Cu and Au arises from the copper support and the sputtered gold film that were employed for characterization. Only C and O can be detected besides Cu and Au, indicating the high purity of the product. XRD pattern reveals the amorphous state of the obtained samples, in agreement with the typically noncrystalline character of activated carbons. Accordingly, no pronounced graphitization occurs under the present carbonization/activation condition. FTIR curve and XPS spectra demonstrate different surface groups on the prepared samples and the assignment of the main signals is as follows on the basis of previous literature.[20] As shown in the FTIR spectrum (Figure

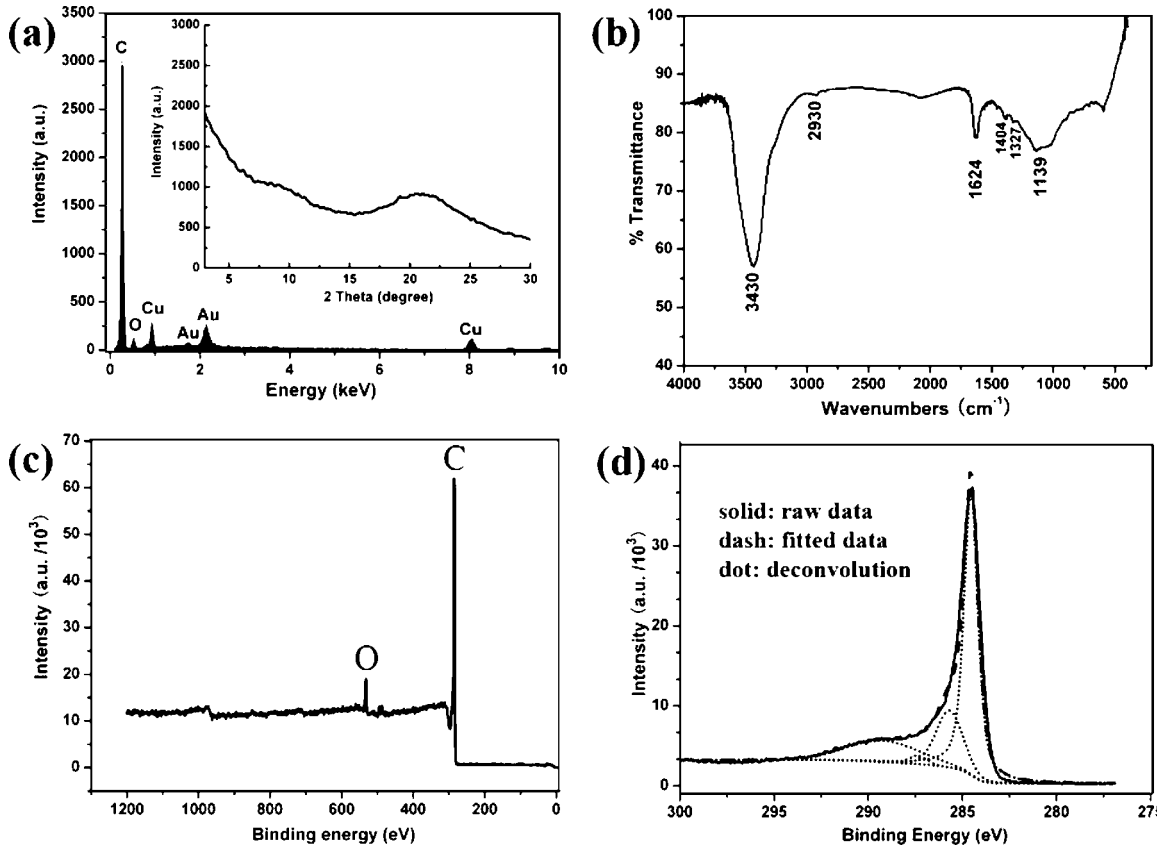

Figure 3. Compositional analysis of sample **BW-D** prepared from biomass waste by carbonization and activation with KOH: (a) EDX spectrum and (inset) powder XRD pattern, (b) FTIR curve, (c) wide XPS spectrum, and (d) refined XPS spectrum of C 1s.

3b), the strongest peak at 3430 cm^{-1} reflects the hydroxy stretching vibration. The weak absorbance at 2930 cm^{-1} can be assigned to aliphatic CH_2 and CH_3 stretch. The sharp peak at 1624 cm^{-1} corresponds to the carboxyl group, while the absorbance bands at 1327 cm^{-1} and 1404 cm^{-1} indicate phenolic structures. The wide absorbance centered at 1139 cm^{-1} is associated with C−O stretch and vibration. The wide XPS spectrum (Figure 3c) confirms the presence of C and O and the absence of other detectable elements, in good agreement with the EDX result. The refined XPS spectrum of C 1s (Figure 3d) reveals the chemical state of carbon. The raw data can be deconvoluted into four separate peaks, demonstrating that carbon of the sample is mainly in an elemental state and partially exists in the form of a carbonyl/carboxyl group. Therefore, the prepared materials are mainly composed of amorphous carbons with different oxygen-containing surface groups. The surface groups on the obtained carbon materials are derived from aromatic structures in lignin precursor, absorbed carbon dioxide and/or moisture, and the surface oxidation of carbon.[20] These carbon−oxygen surface groups may exercise a profound effect on the surface properties of active carbons and thus influence their adsorption characteristics.[21]

The nitrogen sorption isotherms (Figure 4) of the carbon materials derived from biomass waste are of typical type I

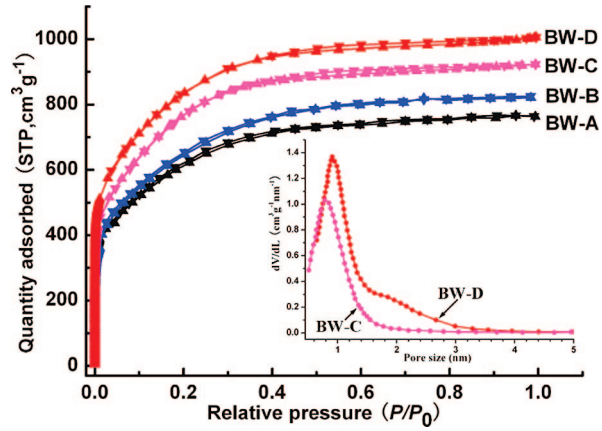

Figure 4. Nitrogen adsorption (up-triangle) and desorption (down-triangle) isotherms of the as-prepared carbon materials, and the pore size distribution (inset) of the **BW-C** and **BW-D** samples.

in the IUPAC classification.[22] A large amount of nitrogen can be adsorbed by all four samples. Very high adsorption of N_2 occurs in a low relative pressure range, and no obvious hysteresis is detected between adsorption and desorption isotherms, indicating the presence of a large proportion of micropores and the absence of macropores or mesopores.[23] Notably, the pore size distributions (PSD, inset of Figure 4) of sample **BW-C** and **BW-D** are relatively narrow. The

(20) Bansal, R. C.; Goyal, M. *Activated Carbon Adsorption*; CRC Press: Boca Raton, 2005.
(21) (a) Jia, X. F.; Xiao, B.; Thomas, K. M. *Langmuir* **2002**, *18*, 470. (b) Xiao, B.; Boudou, J. P.; Thomas, K. M. *Langmuir* **2005**, *21*, 3400.
(22) Rouquerol, J.; Avnir, D.; Fairbridge, C. W.; Everett, D. H.; Haynes, J. H.; Pernicone, N.; Ramsay, J. D. F.; Sing, K. S. W.; Unger, K. K. *Pure Appl. Chem.* **1994**, *66*, 1739.
(23) Gregg, S. J.; Sing, K. S. W. *Adsorption, Surface Area and Porosity*; Academic Press: London, 1982.

Table 1. Yield, Textural Characteristics, and Hydrogen Storage Capacity of the Biomass Waste-Derived Microporous Carbon Materials

sample	yield (%)[a]	surface area (m^2 g^{-1})	total pore volume (cm^3 g^{-1})	maximum distributed pore size (nm)	H_2 uptake (wt %)[b]
BW-A	25.8	2000	1.11	0.77	3.99 (2.03)
BW-B	23.5	2300	1.27	0.80	4.47 (2.21)
BW-C	19.2	2850	1.59	0.85	4.82 (2.39)
BW-D	15.1	3100	1.68	0.91	5.05 (2.55)

[a] Yields of carbon samples are based on the burnoff value of the corresponding hydrolytic precursor. [b] Hydrogen uptake under the pressure of 10 and 1 bar (parentheses) at −196 °C.

dominant pores are in the range of <1.5 nm with the maxima at approximately 0.8 nm. Therefore, the biomass waste-derived active carbons are typically microporous.

Table 1 summarizes the textural properties of the as-synthesized carbons. All samples possess high surface areas exceeding 2000 m^2 g^{-1} and large pore volumes of more than 1 cm^3 g^{-1}, which are comparable to the highest values ever reported for activated carbon materials.[24,25] From sample **BW-A** to **BW-D**, the specific surface area, pore volume, and average pore size increase sequentially with decreasing product yield. The reaction parameters remarkably influence the textures of the obtained carbons. At elevated temperature and prolonged dwell time, more carbon is consumed by the activated reagent, leading to enlarged pores, increased surface areas, and nevertheless lower product yield. Similarly, low yield of **BW-D** is again the result of vigorous carbonization and activation processes applied for the preparation, where volatile matter or carbon contained in the precursors are more prone to be etched by corrosive alkali or intermediate related to it.[26] Texture properties of the samples are consistent with morphology characterization, both demonstrating that the pore structures of biomass-waste derived carbons can be tuned to some extent by adjusting the carbonization and activation parameters. This control of pore size is inferior in accuracy to the case of carbide-derived carbon, which attains a better than 0.05 nm accuracy.[27] However, the production of the present microporous carbons is facile and inexpensive, and meanwhile, they can be employed as representative carbonaceous materials for hydrogen storage study considering the variation of their morphologies and textures.

Figure 5 shows the hydrogen uptake isotherms of the activated carbon materials. No hysteresis is observed in the isotherms, confirming a completely reversible adsorption and desorption of hydrogen by the prepared carbon materials. The H_2 uptake ranges from 2.03 to 2.55 wt % at 1 bar (Table 1), which is higher than the reported data for some typical types of activated carbons possessing lower surface areas[13] and is comparable to that for carbide-derived nanoporous carbons.[17b] An uptake of more than 5 wt % is obtained for

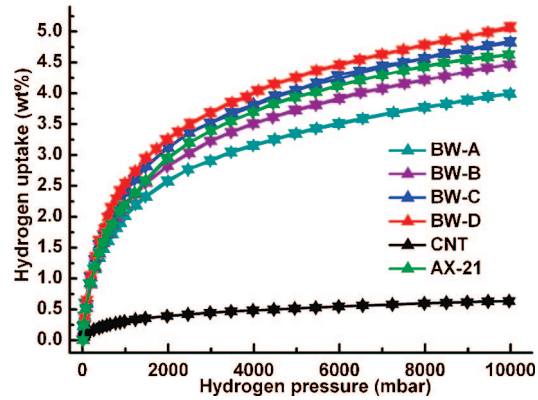

Figure 5. Hydrogen sorption isotherms of the obtained carbons (**BW-A**, **BW-B**, **BW-C**, **BW-D**), AX-21, and multiwalled carbon nanotubes (CNT) at −196 °C over the pressure range of 0–10 bar. Up-triangles and down-triangles represent H_2 adsorption and desorption isotherms, respectively.

sample **BW-D** at 10 bar, close to that of zeolite-like carbon materials (6.9 wt %, 20 bar).[16] H_2 adsorption capacity of commercial activated carbon (AX-21, determined surface area 2800 m^2 g^{-1}) and multiwalled carbon nanotubes (MWCNT, surface area 200 m^2 g^{-1}) were also measured as the comparison and reference. Much lower capacity (0.3 wt % at 1 bar) is demonstrated for MWCNT. The commercial activated carbon AX-21 exhibits a H_2 uptake of 2.1 wt % at 1 bar and 4.6 wt % at 10 bar, which are similar to the results obtained by other groups using a volumetric method[28] and therefore confirm the reliability of our measurement.

In addition, we note that all isotherms display a trend of increasing adsorption with H_2 pressure although the uptake tests can be merely carried out up to 10 bar because of apparatus limitation. Higher hydrogen storage capacity is anticipated under elevated pressures when saturation is attained. Moreover, rapid equilibrium of hydrogen adsorption and desorption can be observed from kinetic data, which show that approximately 99% of the final uptake at a given pressure is achieved within 1 min. Furthermore, we have performed the measurement of H_2 adsorption and desorption isotherms of sample **BW-D** up to 20 cycles and found a favorable cycling capability with total capacity variation less than 1%. Such cyclability may be ascribed to the rigid structure of the synthesized carbons that are capable of enduring the repeated impact during physisorption. Further determination of the hydrogen storage performance from the perspective of volumetric method is now in progress.

A reversible stored amount of hydrogen on carbon materials is believed to be strongly related to the specific surface area and pore size.[9,28a] Our experimental data (Table 1) here indeed reveal a near linear relation between the H_2 uptake and the BET surface area, which is approximately 1 wt % per 1000 $m^2 \cdot g^{-1}$ at −196 °C and 1 bar. Although higher capacity is obtained with higher surface areas, increased deviation from linearity arises, which may be ascribed to different pore size distributions. We also experi-

(24) (a) Alonso, A.; Ruiz, V.; Blanco, C.; Santamaría, M.; Menéndez, R.; deJager, S. G. E. *Carbon* **2006**, *44*, 441. (b) Zhang, F.; Ma, H.; Chen, J.; Li, G. D.; Zhang, Y.; Chen, J. S. *Bioresour. Technol.* **2007**, available online DOI: 10.1016/j.biortech.2007.09.052.
(25) (a) Yang, J.; Shen, Z.; Hao, Z. *Carbon* **2004**, *42*, 1872. (b) Ahmadpour, A.; Do, D. D. *Carbon* **1997**, *35*, 1723.
(26) Guo, J.; Lua, A. C. *J. Colloid Interface Sci.* **2002**, *254*, 227.
(27) Gogotsi, Y.; Nikitin, A.; Ye, H.; Zhou, W.; Fischer, J. E.; Yi, B.; Foley, H. C.; Barsoum, M. W. *Nat. Mater.* **2003**, *2*, 591.
(28) (a) Bénard, P.; Chahine, R. *Langmuir* **2001**, *17*, 1950. (b) Gao, H.; Wu, X. B.; Li, J. T.; Wu, G. T.; Lin, J. Y.; Wu, K.; Xu, D. S. *Appl. Phys. Lett.* **2003**, *83*, 3389. (c) Poirier, E.; Chahine, R.; Bénard, P.; Cossement, D.; Lafi, L. *Appl. Phys. A: Mater. Sci. Process.* **2004**, *78*, 961.

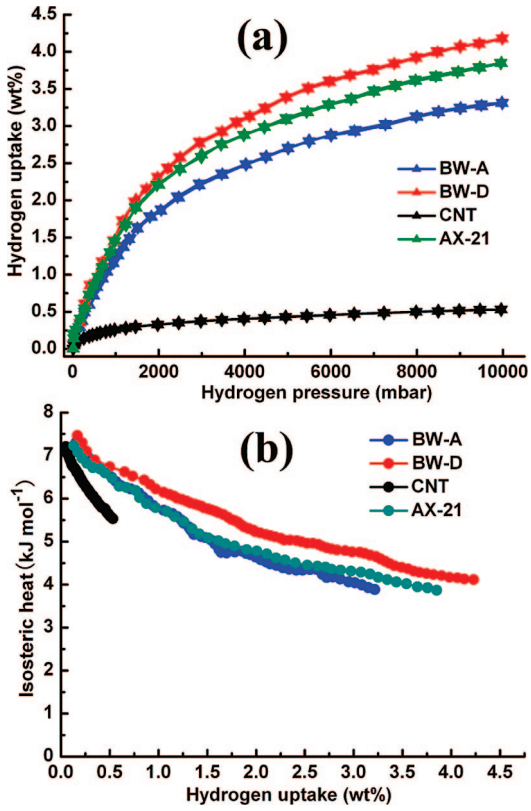

Figure 6. (a) Hydrogen sorption isotherms (up-triangles, adsorption; down-triangles, desorption) measured at −186 °C and (b) isosteric heat of hydrogen adsorption for the biomass waste-derived carbon samples, AX-21, and multiwalled carbon nanotubes.

mentally verify here that the pores below 1 nm contribute significantly to efficient H_2 filling[17b] since the adsorption force increases dramatically with decreased distance of pore walls and hence results in higher compressed gas density.[29] Dominant pore size of the obtained carbon is less than 1 nm. In such micropores, the interaction potential is significantly higher than that in wider pores because of the proximity of the walls, and thus the density and amount of the adsorbed gases are correspondingly enhanced.

To evaluate the interaction between hydrogen and the carbon surface, we have further measured the hydrogen uptake capacity of the carbon samples selectively at liquid argon temperature and calculated the isosteric heat (Q_{st}) of H_2 adsorption (Figure 6). The H_2 sorption isotherms performed at −186 °C exhibit a shape analogous to that taken at −196 °C, although a lower adsorbed amount is displayed. The Q_{st} values vary as a function of hydrogen uptake. Under the same condition, both samples **BW-A** and **BW-D** show higher Q_{st} compared to multiwalled carbon nanotubes. For sample **BW-A**, a slightly weaker H_2−C interaction is observed. This difference in adsorption heat may be attributed to varied parameters such as pore shape or surface chemistry on carbons. For sample **BW-D**, the Q_{st} values range from 4.1 to 7.5 kJ mol^{-1}. The average isosteric heat is comparable to that obtained on zeolite-like carbon materials despite a relatively lower initial value.[16] As to the employed benchmark material (AX-21), the obtained values herein are consistent with previously reported data.[28c] To the best of our knowledge, only carbide derived carbons exhibit apparently higher H_2 heat of adsorption than the present samples among various carbonaceous materials.[17] Therefore, the biomass waste-derived carbons are competitive with the most efficient absorptive materials (e.g., porous carbons and MOFs) in regard to high surface areas, large pore volumes, and strong sorbent−sorbate interaction. These favorable characteristics are responsible for the considerable hydrogen storage capacity of the prepared carbons. Furthermore, a recent work has demonstrated from a thermodynamic perspective that activated carbons are feasible for methane storage and delivery at ambient temperatures.[30] Potential application of the present inexpensive activated carbons in alkane sorption can be expected accordingly.

4. Conclusions

In conclusion, microporous carbon materials with high specific surface areas (2000−3100 m^2 g^{-1}), large micropore volumes, and narrow pore size distribution were facilely prepared from biomass wastes. The as-obtained microporous **BW-D** exhibited considerable cryogenic hydrogen uptake capacities exceeding 5.0 wt % at 10 bar and attaining 2.55 wt % at 1 bar with the adsorption heat of 4.1−7.5 kJ mol^{-1}. The present results thereby indicate that the biomass waste-derived carbons are promising materials for physical adsorption of hydrogen. Furthermore, the prepared inexpensive activated carbons may also find other applications such as in the field of high-efficiency sorption. Therefore, this work would shed light on the more efficient use of biomass wastes with added values.

Acknowledgment. This work was supported by the FP6 Hydrogen Solid Storage Activities (038941) from the European Community and the National NSFC (20701021 & 50771056), MOST Projects (2005CB623607 & 2006AA05Z109), from P.R. China.

CM702816X

(29) Rzepka, M.; Lamp, P.; Casa-Lillo, M. A. *J. Phys. Chem. B* **1998**, *102*, 10894.

(30) Bhatia, S. K.; Myers, A. L. *Langmuir* **2006**, *22*, 1688.